Optical Engineering

SPIEDigitalLibrary.org/oe

Complex degree of mutual anisotropy of biological liquid crystals nets

Yuriy O. Ushenko
Yuriy Ya. Tomka
Igor Z. Misevitch
Vadim V. Istratiy
Olga I. Telenga

SPIE

Complex degree of mutual anisotropy of biological liquid crystals nets

Yuriy O. Ushenko
Chernivtsi National University
Correlation Optics Department
2 Kotsyubinsky Street
Chernivtsi, 58012, Ukraine
E-mail: yuriyu@gmail.com

Yuriy Ya. Tomka
Igor Z. Misevitch
Vadim V. Istratiy
Olga I. Telenga
Chernivtsi National University
Optics and Spectroscopy Department
2 Kotsyubinsky Street
Chernivtsi, 58012, Ukraine

Abstract. This paper is aimed to investigate the potentiality of describing and differentiating optical-anisotropic properties of biological liquid crystal net by statistic analysis of coordinate distributions of a new analytical parameter, a complex degree of mutual anisotropy. [DOI: 10.1117/1.3558850]

Subject terms: polarization; birefringence; liquid crystal; correlation; biological tissue; statistics.

Paper 100956R received Nov. 22, 2010; revised manuscript received Feb. 3, 2011; accepted for publication Feb. 3, 2011; published online Mar. 16, 2011.

1 Brief Theoretical Background for the Technique

Traditionally,[1–18] the processes of forming the polarizationally-heterogeneous fields $U(r)$ were considered in every point (r) as a result of the amplitude (U_x, U_y)–phase (δ) modulation of laser radiation by the biological crystals network

$$\begin{pmatrix} U_x(r) \\ U_y(r) \end{pmatrix} = \begin{Vmatrix} d_{11}(r) & d_{12}(r) \\ d_{21}(r) & d_{22}(r) \end{Vmatrix} \begin{pmatrix} U_{0x} \\ U_{0y}\exp(-i\delta_0) \end{pmatrix} = \begin{pmatrix} d_{11}(r)U_{0x} + d_{12}(r)U_{0y}\exp(-i\delta_0) \\ d_{21}(r)U_{0x} + d_{22}(r)U_{0y}\exp(-i\delta_0) \end{pmatrix}. \quad (1)$$

Here, δ_0 – the phase shift between the orthogonal components U_{0x} and U_{0y} of the illuminating laser beam amplitude; $d_{ik}$is the Jones matrix elements.[1,2]

For the complex analysis of polarizationallyheterogeneous laser radiation fields, a new approach was suggested in Refs. 16, and 19–22, and 23, based on the generalization of the coherence matrix by the polarization coherence matrix for two points (r_1, r_2). In Ref. 16 and 24 for characterizing the consistency between the polarization states of the stationary laser object field in the points (r_1, r_2) with the intensities $I(r_1)$, $I(r_2)$ a new parameter–complex degree of mutual polarization (CDMP) $V(r_1, r_2)$–is introduced. It has the following analytical form:

$$V(r_1, r_2) = 4\frac{\nu_1^2 + \nu_2^2 + \nu_3^2}{I(r_1)\,I(r_2)}, \quad (2)$$

where the coefficients ν_i are determined as the difference of the values of visibility of interference images formed by electromagnetic waves from the points r_1, r_2,

$$\begin{aligned} \nu_1 &= \frac{U_x(r_1)U_x^*(r_2) - U_y(r_1)U_y^*(r_2)}{2}, \\ \nu_2 &= \frac{U_x(r_1)U_y^*(r_2) + U_y(r_1)U_x^*(r_2)}{2}, \\ \nu_3 &= i\frac{U_x(r_1)U_y^*(r_2) - U_y(r_1)U_x^*(r_2)}{2}. \end{aligned} \quad (3)$$

The analysis of coordinate distributions of the CDMP polarization-heterogeneous laser images of biological liquid crystals net, protein fibrils network forming the biological tissue (BT) extracellular matrix, became an important diagnostic application of the above-mentioned theoretical approach. The ranges of changes of the 1stto the 4th order statistic moments of coordinate distributions of the CDMP of the corresponding laser images, important for diagnostics of the human connective tissue oncologic state, were determined in Refs. 2 and 16. On the other hand, such analysis leads to disregarding the BT extracellular matrix birefringence, which is a principal physical mechanism of their polarizationally-heterogeneous images formation. That is why it appears to be important to search for new diagnostic parameters directly characterizing the degree of consistency of optical axes and birefringence orientations of various points of BT liquid crystal net.[6,9,12,13] Further, similarly to Ref. 24, we shall call such a parameter the complex degree of mutual anisotropy (CDMA).

Taking into account Eqs. (1)–(3) we obtain the expression of CDMA $W(r_1, r_2)$ of two points (r_1, r_2) of the biological liquid crystal

$$W(r_1, r_2) = \frac{\{[d_{11}(r_1) + id_{12}(r_1)][d_{11}(r_2) + id_{12}(r_2)]^* + [d_{21}(r_1) + id_{22}(r_1)][d_{21}(r_2) + id_{22}(r_2)]^*\}^2}{I(r_1)\,I(r_2)}. \quad (4)$$

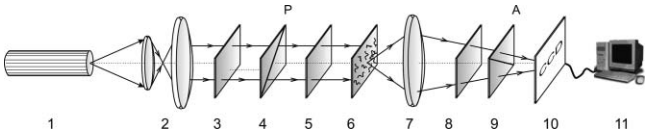

Fig. 1 Optical scheme of polarimeter for measuring coordinate CDMA distributions Here 1 is the He-Ne laser ($\lambda = 0.6328$ μm); 2 is the collimator; 3, 5 and 8 are the quarter-wave plates; 4 and 9, are the polarizers; 6 are the BT histological section; 7 are the projection microobjective; 10 is the CCD –camera; 11 is the PC.

The operation of complex conjugation is designated by the asterisk $(*)$.

2 Diagnostic Possibilities of Investigations of 2-D Distributions of the CDMA

Experimental investigations were carried out in the classical polarimeter, the main parts and elements of which are presented in Fig. 1.[2] The value of CDMA $W(r_1, r_2 = r_1 + \Delta r)$ of the two points $(r_1, r_1 + \Delta r)$ shifted by the interval Δr of the network of protein liquid crystals is calculated using Eq. (4). Coordinate distribution $W(x, y)$ of the BT layer extracellular matrix is determined by scanning with the $\Delta r = 1$ pix step in two mutually transverse directions $(x = 1 \div m, y = 1 \div n)$. Here m, n is the quantity of CCD camera pixels.

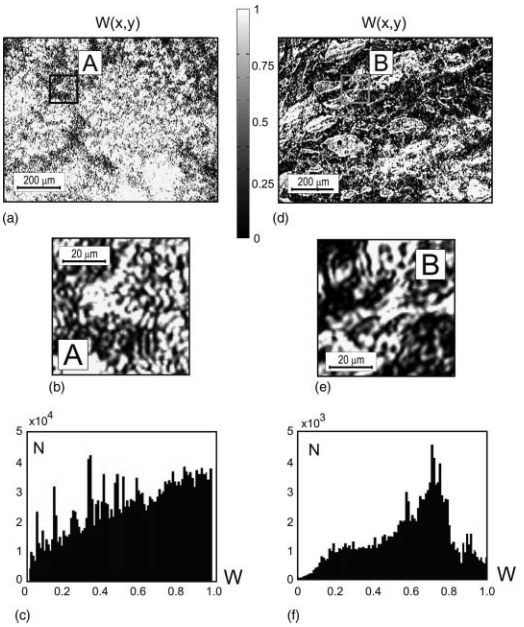

Fig. 2 Coordinate distributions [600 pix×800 pix – fragments (a), (d); 50 pix×50 pix – fragments (b), (e)] and histograms [fragments (c), (f)] of values $W(x, y)$ of physiologically normal.

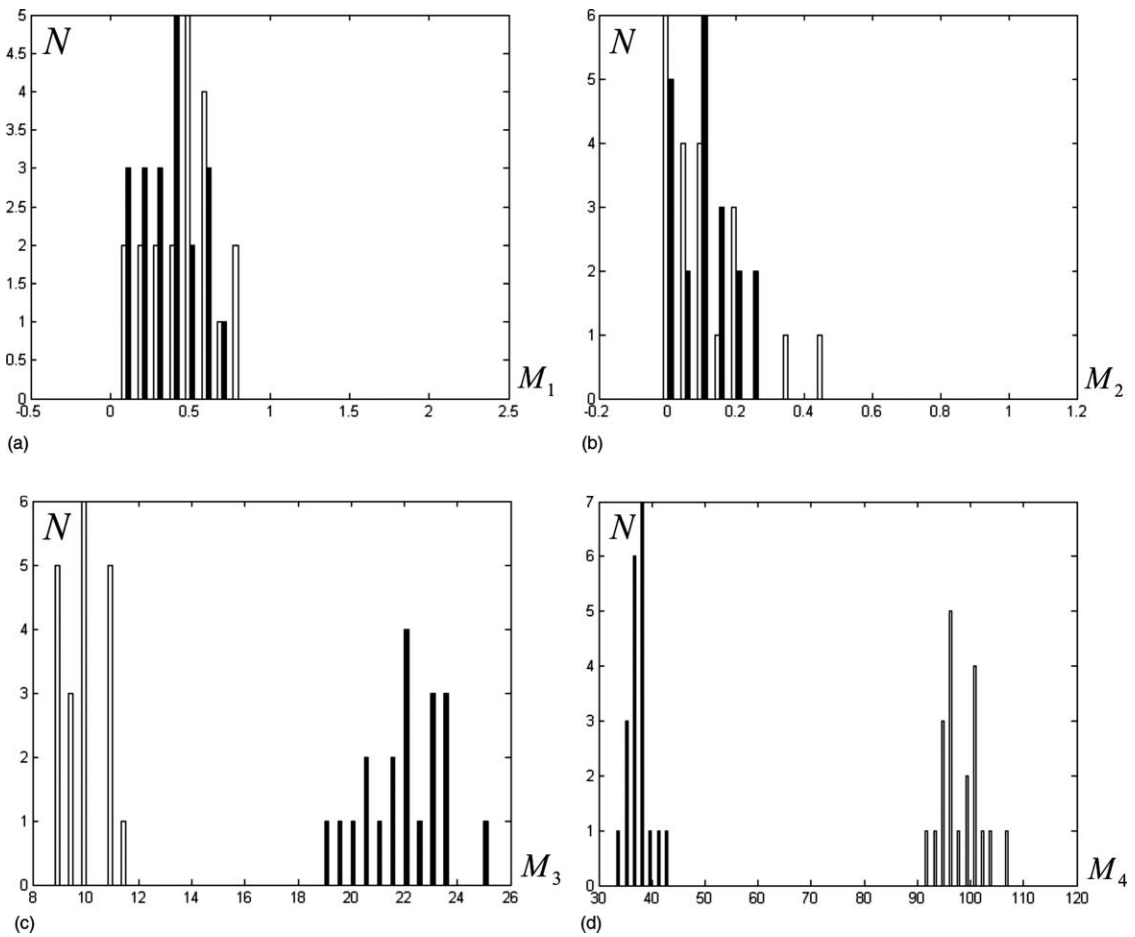

Fig. 3 The histograms of statistical moments of CDMA $W(x, y)$ for physiologically normal (white bars) and pathologically changed (black bars) connective tissue.

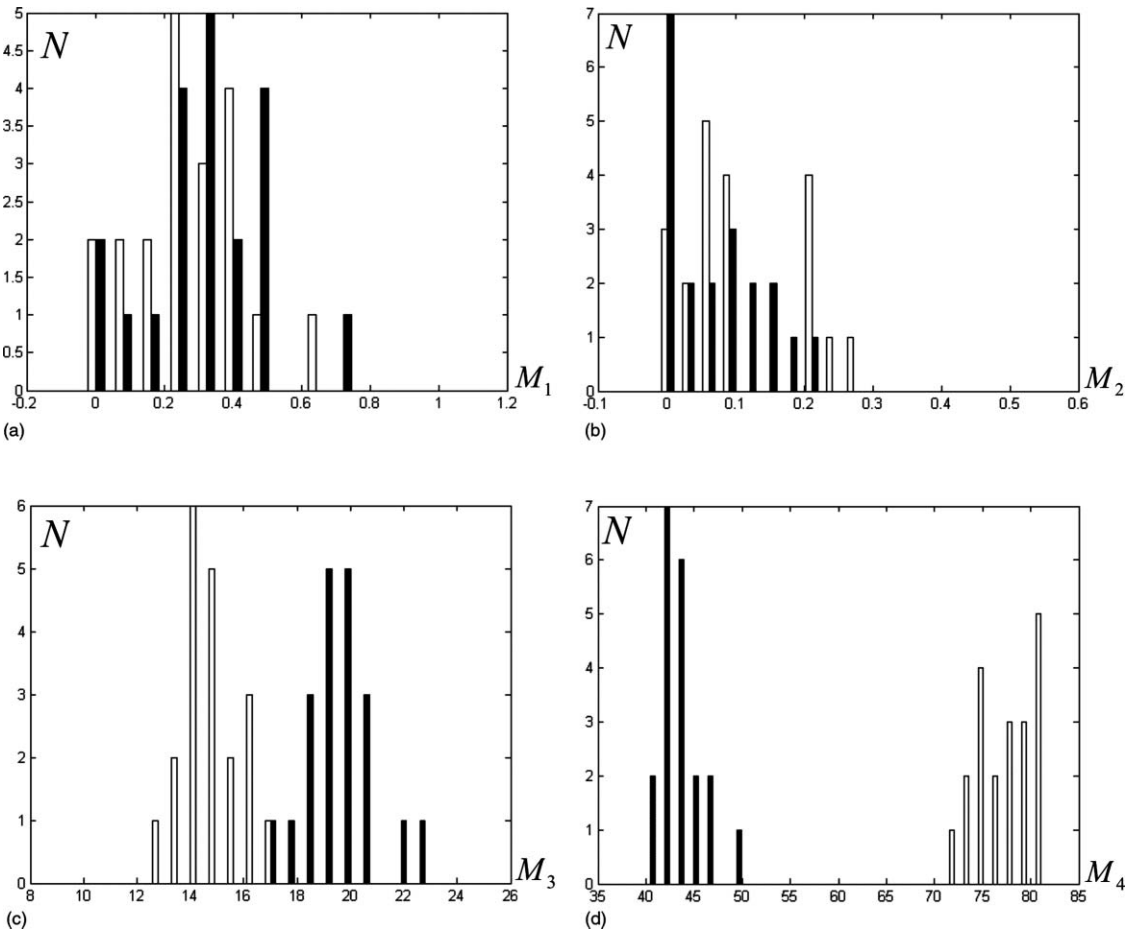

Fig. 4 The histograms of statistical moments of CDMP $V(x, y)$ for physiologically normal (white bars) and pathologically changed (black bars) connective tissue.

The optically thin (the attenuation coefficient $\tau < 0.1$) histological sections of sound connective tissue ($k = 20$ samples) and oncologically changed (k = 19 samples) one (dysplasia – pre-cancer state) of uterus neck were taken as the objects of investigation.

The series of coordinate distributions [600 pix × 800 pix, fragments (a), (d); 50 pix × 50 pix, fragments (b), (e)] and the histograms [fragments (c), (f)] of CDMA values $\tilde{W}(x, y)$ of physiologically normal [fragments (a), (b), (c)] and pathologically changed [fragments (d), (e), (f)] connective tissue samples are presented in Fig. 2.

For a chaotically oriented network of liquid crystals of the sound tissue extracellular matrix [Figs. 2(a) and 2(b)], the values of $W(x, y)$ histograms represent rather equiprobable distributions [Fig. 2(c)]. Early oncologic changes of connective tissue are accompanied with the formation of the protein liquid crystals net growth direction. It is optically shown [Figs. 2(d) and 2(e)], in some localization of the CDMA random values distribution [Fig. 2(f)] in the domain of $W = 0,5 \div 0,75$ extrema.

In order to obtain objective criteria of diagnostic efficiency, the comparative investigation of CDMP $[V(x, y)]$ and CDMA $W(x, y)$ techniques was performed in the conditions of single and multiple scattering of laser radiation by the layers of uterus neck connective tissue. In order to form single and multiple scattering regimes, we have used histological sections of biological tissues with different geometric thicknesses (15 and 40 μm).

In Figs. 3 and 4, the comparative results of calculations of the average (M_1), the dispersion (M_2), the skewness (M_3), and the kurtosis (M_4) of CDMA $W(x, y)$ (Fig. 3) distributions of two groups of connective tissue and of CDMP $V(x, y)$ (Fig. 4) of their laser images are presented. In order to estimate the statistic reliability of calculations, the amount of samples within each group (norm or oncology) were chosen so that the confidence interval is $p < 0.01$. The area of the illuminating laser beam was so chosen that magnitudes of M_1, M_2, M_3, and M_4 did not depend on displacement in the plane of the histological section sample. For our experiment, the diameter of the laser beam was 5 mm, and the size of the histological section was 15 × 15 mm.

The statistic moments were calculated in accordance with the following technique:[15,16]

$$M_1 = \frac{1}{N}\sum_{i=1}^{N} |W(x, y)|,\ M_2 = \sqrt{\frac{1}{N}\sum_{i=1}^{N} [W(x, y) - M_1]_i^2},$$

$$M_3 = \frac{1}{M_2^3}\frac{1}{N}\sum_{i=1}^{N} W(x, y)_i^3,\ M_4 = \frac{1}{M_2^4}\frac{1}{N}\sum_{i=1}^{N} W(x, y)_i^4, \tag{5}$$

where N is the number of elements in discrete sampling.

From the obtained data about the coordinate distributions of CDMA of optically thin layers of connective tissue, one can see that:

- The average and dispersion of distributions $W(x, y)$ of both types of samples differ insufficiently. For 2-D distributions $V(x, y)$ of laser images, there is practically no difference between M_1 and M_2.
- The skewness values M_3 of distributions $W(x, y)$ of the investigated samples differ by 2.1 times; the kurtosis values by 3.2 times. For CDMP distributions $V(x, y)$, the values of the 3rd and 4th statistic moments vary for M_3 by 1.3 times; for M_4 by 1.8 times.

3 Conclusion

To characterize the degree of consistency of parameters of the optically uniaxial birefringent protein liquid crystal nets of BT a new parameter, a complex degree of mutual anisotropy is suggested. The technique of polarization measuring the coordinate distributions of the complex degree of mutual anisotropy of BT is developed. It is shown that a statistic approach to the analysis of distributions $W(x, y)$ of BT of various optical thicknesses appears to be more sensitive and efficient in the differentiation of their physiological state in comparison with investigations of complex degree of mutual polarization of the corresponding laser images.

References

1. M. Born and E. Wolf, *Principles of Optics*, Cambridge University Press, Cambridge (1999).
2. A. G. Ushenko and V. P. Pishak, "Laser plarimetry of biological tissue: principles and applications," in *Handbook of Coherent-Domain Optical Methods: Biomedical Diagnostics, Environmental and Material Science*, Valery V. Tuchin, Ed., pp. 93–138, Kluwer Academic, New York (2004).
3. A. G. Ushenko, "Polarization structure of laser scattering fields," *Opt. Eng.* **34**(4), 1088–1093 (1995).
4. A. G. Ushenko, "Laser diagnostics of biofractals," *Quantum Electron.* **29**(12), 1078–1084 (1999).
5. O. V. Angel'skii, A. G. Ushenko, A. D. Arkhelyuk, S. B. Ermolenko, and D. N. Burkovets, "Structure of matrices for the transformation of laser radiation by biofractals," *Quantum Electron*. **29**(12), 1074–1077 (1999).
6. O. V. Angel'skii, A. G. Ushenko, A. D. Arheluk, S. B. Ermolenko, and D. N. Burkovets, "Scattering of laser radiation by multifractal biological structures," *Opt. Spectrosc.* **88**(3), 444–448 (2000).
7. A. G. Ushenko, "Polarization structure of biospeckles and the depolarization of laser radiation," *Opt. Spectrosc.* **89**(4), 597–601 (2000).
8. A. G. Ushenko, "Stokes-correlometry of biotissues," *Laser Phys.* **10**(5), 1286–1292 (2000).
9. A. G. Ushenko, "The vector structure of laser biospeckle fields and polarization diagnostics of collagen skin structures," *Laser Phys.* **10**(5), 1143–1149 (2000).
10. A. G. Ushenko, "Laser polarimetry of polarization-phase statistical moments of the object field of optically anisotropic scattering layers," *Opt. Spectrosc.* **91**(2), 313–316 (2001).
11. A. G. Ushenko, "Polarization contrast enhancement of images of biological tissues under the conditions of multiple scattering," *Opt. Spectrosc.* **91**(6), 937–940 (2001).
12. A. G. Ushenko, "Laser probing of biological tissues and the polarization selection of their images," *Opt. Spectrosc.* **91**(6), 932–936 (2001).
13. A. G. Ushenko, "Correlation processing and wavelet analysis of polarization images of biological tissues," *Opt. Spectrosc.* **91**(5), 773–778 (2002).
14. A. G. Ushenko, "Polarization correlometry of angular structure in the microrelief pattern or rough surfaces," *Opt. Spectrosc.* **92**(2), 227–229 (2002).
15. O. V. Angelsky, A. G. Ushenko, and Y. G. Ushenko, "2-D Stokes polarimetry of biospeckle tissues images in pre-clinic diagnostics of their pre-cancer states," *J. Holography Speckle* **2**(1), 26–33 (2005).
16. O. V. Angelsky, A. G. Ushenko, and Y. G. Ushenko, "Complex degree of mutual polarization of biological tissue coherent images for the diagnostics of their physiological state," *J. Biomed. Opt.* **10**(6), 060502 (2005).
17. O. V. Angelsky, A. G. Ushenko, and Ye. G. Ushenko, "Investigation of the correlation structure of biological tissue polarization images during the diagnostics of their oncological changes," *Phys. Med. Biol.* **50**, 4811–4822 (2005).
18. O. V. Angelsky, A. G. Ushenko, Y. G. Ushenko, and Y. Y. Tomka, "Polarization singularities of biological tissues images," *J. Biomed. Opt.* **11**(5), 054030 (2006).
19. F. Gori, M. Santarsiero, S. Vicalvi, R. Borghi, and G. Guattari, "Beam coherence-polarization matrix," *Pure Appl. Opt.* **7**, 941–951 (1998).
20. F. Gori, "Matrix treatment for partially polarized, partially coherent beams," *Opt. Lett.* **23**, 241–243 (1998).
21. E. Wolf, "Unified theory of coherence and polarization of random electromagnetic beams," *Phys. Lett. A.* **312**, 263–267 (2003).
22. M. Mujat and A. Dogariu, "Polarimetric and spectral changes in random electromagnetic fields," *Opt. Lett.* **28**, 2153–2155 (2003).
23. J. Ellis, A. Dogariu, S. Ponomarenko, and E. Wolf, "Interferometric measurement of the degree of polarization and control of the contrast of intensity fluctuations," *Opt. Lett.* **29**, 1536–1558 (2003).
24. J. Ellis and A. Dogariu, "Complex degree of mutual polarization," *Opt. Lett.* **29**, 5365–5338 (2004).

Biographies and photographs of the authors not available.